Sphingosine 1-phosphate rapidly increases endothelial barrier function independently of VE-cadherin but requires cell spreading and Rho kinase

Mei Xu, Chris L. Waters, Chuan Hu, Robert B. Wysolmerski, Peter A. Vincent and Fred L. Minnear

Am J Physiol Cell Physiol 293:1309-1318, 2007. First published Aug 1, 2007;
doi:10.1152/ajpcell.00014.2007

Am J Physiol Cell Physiol 293: C1309–C1318, 2007.
First published August 1, 2007; doi:10.1152/ajpcell.00014.2007.

Sphingosine 1-phosphate rapidly increases endothelial barrier function independently of VE-cadherin but requires cell spreading and Rho kinase

Mei Xu,[1] Chris L. Waters,[1] Chuan Hu,[1,2] Robert B. Wysolmerski,[1,3] Peter A. Vincent,[4] and Fred L. Minnear[1,2]

[1]*Center for Interdisciplinary Research in Cardiovascular Sciences,* [2]*Department of Physiology and Pharmacology, and* [3]*Department of Neurobiology and Anatomy, West Virginia University School of Medicine, Morgantown, West Virginia; and* [4]*Center for Cardiovascular Sciences, Albany Medical College, Albany, New York*

Submitted 10 January 2007; accepted in final form 13 July 2007

Xu M, Waters CL, Hu C, Wysolmerski RB, Vincent PA, Minnear FL. Sphingosine 1-phosphate rapidly increases endothelial barrier function independently of VE-cadherin but requires cell spreading and Rho kinase. *Am J Physiol Cell Physiol* 293: C1309–C1318, 2007. First published August 1, 2007; doi:10.1152/ajpcell.00014.2007.—Sphingosine 1-phosphate (S1P) rapidly increases endothelial barrier function and induces the assembly of the adherens junction proteins vascular endothelial (VE)-cadherin and catenins. Since VE-cadherin contributes to the stabilization of the endothelial barrier, we determined whether the rapid, barrier-enhancing activity of S1P requires VE-cadherin. Ca^{2+}-dependent, homophilic VE-cadherin binding of endothelial cells, derived from human umbilical veins and grown as monolayers, was disrupted with EGTA, an antibody to the extracellular domain of VE-cadherin, or gene silencing of VE-cadherin with small interfering RNA. All three protocols caused a reduction in the immunofluorescent localization of VE-cadherin at intercellular junctions, the separation of adjacent cells, and a decrease in basal endothelial electrical resistance. In all three conditions, S1P rapidly increased endothelial electrical resistance. These findings demonstrate that S1P enhances the endothelial barrier independently of homophilic VE-cadherin binding. Junctional localization of VE-cadherin, however, was associated with the sustained activity of S1P. Imaging with phase-contrast and differential interference contrast optics revealed that S1P induced cell spreading and closure of intercellular gaps. Pretreatment with latrunculin B, an inhibitor of actin polymerization, or Y-27632, a Rho kinase inhibitor, attenuated cell spreading and the rapid increase in electrical resistance induced by S1P. We conclude that S1P rapidly closes intercellular gaps, resulting in an increased electrical resistance across endothelial cell monolayers, via cell spreading and Rho kinase and independently of VE-cadherin.

permeability; microscopy; electric cell-substrate impedance sensing; human umbilical vein endothelial cell

VASCULAR ENDOTHELIA act as a restrictive barrier and as such regulate many biological processes such as protein and fluid transport, inflammation, white cell emigration, and angiogenesis. Disruption of the endothelial barrier leads to accumulation of fluid and macromolecules in the interstitial space, resulting in edema and dysfunction of tissues and organs (1, 11, 14). The cellular mechanism(s) that regulates the endothelial barrier is not known and may involve a number of cellular processes. Proposed mechanisms include alterations in the integrity of the junctions, the cytoskeleton, and focal adhesions and cellular retraction/contraction and relaxation (1, 11, 14). Tight junctions comprised of occludins, claudins, ZO-1, etc. impart the barrier characteristics of epithelial cells; however, their importance with respect to endothelial barrier function requires further study (1). The endothelial adherens junction, containing vascular endothelial (VE)-cadherin, other cadherins, and catenins, has been studied extensively, and modifications to VE-cadherin profoundly affect the integrity of the endothelial barrier. For example, antibodies directed toward the extracellular domain of VE-cadherin increased permeability of endothelial cell monolayers (4) and vascular permeability in heart and lungs of mice (5).

Sphingosine 1-phosphate (S1P) is a biologically active lipid released from a number of cells, notably platelets, and is present in blood and serum at nanomolar to micromolar concentrations. S1P enhances the barrier function of cell monolayers (8), prevents the increase in hydraulic conductivity induced by platelet-activating factor in single venular microvessels (17), and attenuates the increase in pulmonary edema in mice and dogs subjected to intratracheal endotoxin (12, 19). In addition, S1P enhances the localization of VE-cadherin and α-, β-, and γ-catenins at endothelial junctions within 30–60 min of treatment (9, 13). S1P has also been shown to induce membrane ruffling and cell spreading of single endothelial cells (6, 18) and lamellipodia formation and cell spreading at the leading edge of wounded endothelial cell monolayers (25). Cell spreading is also induced by cAMP-enhancing agents that are well known to rapidly tighten the endothelial barrier (15, 22).

Therefore, the primary objective of the present study was to delineate the involvement of homophilic VE-cadherin binding and cell spreading in the enhancement of endothelial barrier function induced by S1P. VE-cadherin binding was disrupted with three different methodologies, addition of EGTA to the cell culture medium to lower extracellular Ca^{2+}, addition of an antibody to the extracellular domain of VE-cadherin, and gene silencing of VE-cadherin with small interfering RNA (siRNA). Imaging of live cells by phase-contrast and differential interference contrast (DIC) optics documented changes in cell shape. Evidence of closure of intercellular gaps, induced by the treatment of EGTA, was demonstrated microscopically and by an increase in endothelial electrical resistance. Since actin polymerizes at the leading edge of spreading cytoplasm (21), S1P reorganizes actin to the cell periphery (8), and activation of the small GTPase Rho has been implicated in the spreading of single endothelial cells by S1P (18), we further determined

Address for reprint requests and other correspondence: F. L. Minnear, Dept. of Physiology and Pharmacology, PO Box 9229, Robert C. Byrd Health Sciences Center, West Virginia Univ., Morgantown, WV 26506 (e-mail: fminnear@hsc.wvu.edu).

The costs of publication of this article were defrayed in part by the payment of page charges. The article must therefore be hereby marked "*advertisement*" in accordance with 18 U.S.C. Section 1734 solely to indicate this fact.

whether inhibitors of actin polymerization and Rho kinase, an effector of Rho, would impede the spreading of endothelial cells by S1P.

MATERIALS AND METHODS

Materials. S1P was purchased from Avanti Polar Lipids (Alabaster, AL). Gentamicin sulfate was from ICN Biomedicals (Aurora, OH). Newborn calf serum and bovine brain extract were from Cambrex (East Rutherford, NJ). Prolong Gold antifade reagent, Alexa Fluor-labeled secondary antibodies, and Alexa Fluor-labeled phalloidin were from Invitrogen-Molecular Probes (Eugene, OR). Gold-coated cell-substrate impedance sensing (ECIS) electrodes were from Applied Biophysics (Troy, NY). Rabbit anti-human VE-cadherin antibodies were purchased from US Biological (Swampscott, MS) and Axxora (San Diego, CA). Goat anti-human VE-cadherin antibody and normal rabbit IgG were from Santa Cruz Biotechnology (San Diego, CA). Horseradish peroxidase-conjugated secondary antibodies were purchased from Chemicon International (Temecula, CA). Control (scrambled) siRNA and VE-cadherin siRNA (Smartpool) were from Dharmacon (Chicago, IL). Nitrocellulose membranes and enhanced chemiluminescence (ECL) Western blotting detection reagents were from Amersham Biosciences (Little Chalfont, UK). All other chemicals were from Sigma-Aldrich (St. Louis, MO).

Cell culture. Endothelial cells from human umbilical veins (HUVECs) were isolated with 1 mg/ml of type I collagenase and grown in MCDB-131 (MCDB) culture medium containing 5% (vol/vol) human serum, 20% (vol/vol) newborn calf serum, 7.5 μg/ml endothelial cell growth supplement, 4.5 μg/ml bovine brain extract, 25 μg/ml porcine intestinal heparin, and 50 μg/ml gentamicin sulfate. HUVECs (*passages 2–8*) were grown to confluence (2 days) in a humidified incubator maintained at 37°C and 5% CO_2. Before treatment with S1P, MCDB containing 25% serum was replaced with serum-free MCDB, and the cell monolayers were allowed to equilibrate for 2 h in an incubator.

Transendothelial electrical resistance. To assess changes in endothelial barrier function, electrical resistance was measured continuously across HUVEC monolayers by ECIS (7, 16). Briefly, HUVECs (80,000–100,000 cells) were seeded onto ECIS cultureware (0.8 cm^2/well) precoated with 0.2% gelatin. The electrical resistance measured was that of those cells located on the small gold electrode (5×10^{-4} cm^2) in each of the wells. The culture medium was the electrolyte, and the small gold electrode, covered by confluent endothelial cells, and a larger gold counterelectrode (~2 cm^2) were connected to a phase-sensitive lock-in amplifier. A constant current of 1 μA was supplied by a 1-V, 4,000-Hz alternating current through a 1-MΩ resistor. Changes in voltage between the small electrode and the large counterelectrode were monitored by the lock-in amplifier, stored, and then calculated as resistance by the computer. The small size of the cell-seeded electrode is the critical feature of the system. When electrodes of $\leq 10^{-3}$ cm^2 are used, the impedance at the small electrode dominates the system, allowing for assessment of the morphological changes of the cells located at this interface. Electrical resistance of the bare electrode is ~2,000 Ω and increases to ≥10,000 Ω when HUVECs have become confluent. If the electrical resistance of the endothelial cell-covered electrode is 10,000 Ω, as depicted in Fig. 4, and is corrected for electrical resistance of the bare electrode (2,000 Ω), then multiplying 8,000 Ω times the electrode surface area of 5×10^{-4} cm^2 yields a basal electrical resistance across the HUVEC monolayer of 4 Ω·cm^2, similar to 5 Ω·cm^2 as reported with a Ussing-type recording chamber (24).

EGTA protocol. HUVEC monolayers were treated with 2 mM ethylene glycol-bis(β-aminoethyl ether)-*N,N,N′,N′*-tetraacetic acid (EGTA) for 10 min to chelate extracellular Ca^{2+}, followed by *1*) no treatment, *2*) addition of 400 μl of fresh MCDB containing 1.6 mM Ca^{2+} to restore extracellular Ca^{2+}, *3*) addition of only 1 μM S1P (in 1 μl) without restoration of extracellular Ca^{2+} or *4*) addition of S1P and MCDB together. For *treatments 1* and *3*, EGTA was present in the cell culture medium for the entire experimental period. For *treatments 2* and *4*, culture medium was withdrawn at 10 min after the administration of EGTA and before the addition of fresh MCDB. S1P was solubilized in methanol with sonication and transferred to microcentrifuge tubes (0.5 ml). Methanol was subsequently removed by nitrogen, and the tubes with S1P were stored at −20°C. S1P was reconstituted in 1× Tris-buffered saline (TBS) diluted from 1 M Tris·HCl (pH 8.0) for experimentation. Reconstitution of S1P in TBS plus 0.4% fatty acid-free albumin yielded similar results. Control solutions, TBS alone, or TBS plus albumin had no effect on basal endothelial electrical resistance.

Immunofluorescence confocal microscopy. After the various treatments, HUVEC monolayers were rinsed with phosphate-buffered saline containing Ca^{2+} and Mg^{2+} (PBS+/+). Cells were fixed with 3.7% paraformaldehyde for 15 min, permeabilized for 5 min in cytoskeletal buffer (in mM: 10 PIPES at pH 6.8, 3 $MgCl_2$, 100 NaCl, and 300 sucrose) containing 0.5% Triton X-100, and then incubated for 20 min with 5% BSA. Rabbit anti-human VE-cadherin polyclonal antibody was added to the cells for 60 min, followed by Alexa Fluor 488- or 594-labeled goat anti-rabbit IgG and Alexa Fluor 488-labeled phalloidin to identify actin filaments, and the cells were rinsed several times with PBS+/+. Cells were mounted with Prolong Gold antifade reagent. Images were generated by confocal laser scanning with a Zeiss LSM 510 confocal microscope. When comparing images, the fluorescent signals were measured at emission wavelengths of 488 and 594 nm with the same pinhole (<1 μm), the same detector gain, and the same amplifier offset.

RNA interference. VE-cadherin siRNA was transiently transfected into HUVECs by electroporation with the Nucleofector I device (Amaxa Biosystems, Berlin, Germany). Briefly, 90% confluent cell monolayers were trypsinized and individual cells were counted. After centrifugation, 1.5×10^6 cells were resuspended in 100 μl of a Nucleofector solution (in mM: 7.25 ATP, 12 $MgCl_2 \cdot 6H_2O$, 88 KH_2PO_4, 14 $NaHCO_3$, and 2 glucose at pH 7.4) with 400 pmol of VE-cadherin siRNA or control scrambled siRNA. The cells in solution were transferred immediately to a cuvette and electroporated in the Nucleofector apparatus with the U-01 program. Transfected cells were recovered with warm fresh MCDB for 5 min, seeded immediately on 0.2% gelatin-coated ECIS wells, monitored for electrical resistance, or seeded on 24-well tissue culture plates and placed in an incubator for 2 days until being used for microscopy or Western blot experiments. The protein level of VE-cadherin was quantified from Western blots by densitometry after normalization to β-actin as a protein loading control.

Immunoblotting. Cells were washed twice in ice-cold PBS, lysed in RIPA buffer (15 mM NaCl, 50 mM Tris, 1% NP-40, and 0.5% sodium deoxycholate) containing 2 mM EGTA, phosphatase inhibitors (1 mM sodium vanadate and 1 mM phenylmethylsulfonyl fluoride), and proteinase inhibitors (5 μg/ml aprotinin and 2 μg/ml leupeptin). Samples were clarified by centrifugation at 14,000 rpm for 10 min at 4°C. Proteins were resolved by sodium dodecyl sulfate-polyacrylamide gel electrophoresis (SDS-PAGE) and transferred to nitrocellulose membrane with a mini-Protean electrophoresis system. Protein blots were probed with indicated primary antibodies, followed by the appropriate horseradish peroxidase-conjugated secondary antibody, and developed by ECL.

Cell spreading. HUVECs were grown to confluence in 35-mm glass-bottom culture dishes or Delta T culture dishes. Cells were placed in serum-free MCDB with 20 mM HEPES for 2 h. For phase-contrast microscopy, 35-mm glass-bottom dishes were inserted into a temperature (37°C)- and humidity-controlled chamber mounted on the stage of a Zeiss AxioVert 200M microscope, and cells were viewed through a ×20 phase-contrast objective and ×1.6 Optovart to increase magnification. For DIC microscopy, Delta T culture dishes with a temperature-controlled bottom were placed on the stage of a Nikon Eclipse TE 2000-5 microscope, and cells were viewed through

a ×20 DIC optical lens. Phase-contrast images were obtained with a Zeiss AxioCam camera and Axiovision software, and DIC images were processed with a Nikon camera and Metamorph software.

Statistics. All values are presented as means ± SE. A minimum of three experiments were conducted for ECIS experiments and five for microscopy experiments. Data on electrical resistance were analyzed with a two-way analysis of variance with repeated measures (26). Differences between treatments at specific time points were analyzed further with a Bonferroni posttest. Statistical significance was set at $P < 0.05$.

RESULTS

S1P rapidly increased endothelial electrical resistance independently of homophilic VE-cadherin binding. S1P has been reported to increase the localization of VE-cadherin at intercellular junctions (9, 13). To determine whether this increase is responsible for the rapid increase in endothelial electrical resistance induced by S1P, homophilic VE-cadherin binding was disrupted by three different protocols: *1*) addition to the culture medium of 2 mM EGTA to chelate extracellular Ca^{2+}, *2*) addition of an antibody to the extracellular domain of VE-cadherin, and *3*) gene silencing of VE-cadherin. In all three protocols, S1P (1 μM) rapidly increased electrical resistance across endothelial cell monolayers in association with a reduction in the localization of VE-cadherin at intercellular junctions.

Addition of EGTA to the cell culture medium caused a precipitous decrease in endothelial electrical resistance (Fig. 1*A*) and a loss of VE-cadherin at intercellular junctions (Fig. 2*A*). After 10 min of incubation with EGTA, cell monolayers were either not treated or treated with MCDB (containing 1.6 mM) to replenish extracellular Ca^{2+}, S1P alone (1 μM in 1 μl), or MCDB plus S1P. Therefore, cell monolayers not treated or treated with S1P alone were exposed to EGTA for the entire experimental period, whereas cell monolayers treated with MCDB or S1P plus MCDB were exposed to concentrated EGTA for only 10 min. Endothelial electrical resistance did not change with no treatment and increased slightly and then slowly returned to the pre-EGTA level with the addition of MCDB (Fig. 1). In contrast, electrical resistance increased rapidly within 10 min to the pre-EGTA level or above on treatment with S1P without or with MCDB, respectively (Fig. 1). The identical EGTA protocol was repeated to visualize VE-cadherin and filamentous actin (F-actin) by confocal microscopy (Fig. 2). A characteristic of the S1P response is a reorganization of actin to the cell periphery (8), which was also observed in the present study within 10 min of treatment with S1P or S1P plus MCDB subsequent to the addition of EGTA (Fig. 2*A*). In control cell monolayers, VE-cadherin appeared prominently at intercellular junctions. Twenty minutes (also 10 min, data not shown) after EGTA treatment, there was a reduction in junctional VE-cadherin and an apparent increase in VE-cadherin in the cytoplasm (Fig. 2*A*). In addition, gaps were present between adjacent cells. After replacement of extracellular Ca^{2+} with the addition of fresh MCDB, VE-cadherin was observed to some extent at intercellular junctions and there was a reduction in cytoplasmic VE-cadherin within 10 min (Fig. 2*A*). The effect of S1P on junctional VE-cadherin was dependent on whether MCDB was added to restore extracellular Ca^{2+}. After treatment with S1P alone for 10 min, very little VE-cadherin was observed at intercellular junctions. On

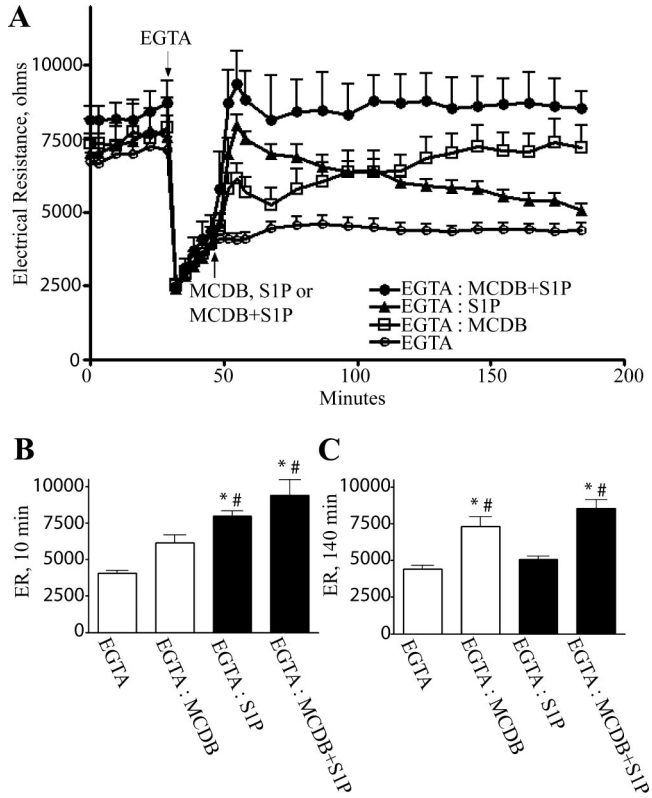

Fig. 1. Sphingosine 1-phosphate (S1P) rapidly increased endothelial electrical resistance after chelation of extracellular Ca^{2+} with EGTA. Ca^{2+} in culture medium of cell monolayers derived from human umbilical vein endothelial cells (HUVECs) was chelated with 2 mM EGTA. Cells were then not treated (EGTA, ○) or treated (arrow) with MCDB-131 (MCDB, □) to restore extracellular Ca^{2+}, S1P alone (1 μM in 1 μl, ▲), or S1P + MCDB (●). EGTA-containing medium was removed before addition of MCDB without or with S1P but remained for cell monolayers not treated or treated with S1P alone. *A*: continuous data recorded over 180-min time period. *B*: values at 10 min after treatments with MCDB, S1P, or MCDB + S1P. *C*: values at 140 min after treatments. Note that S1P rapidly increased endothelial electrical resistance (ER) without or with addition of MCDB (*A*, *B*), whereas sustained activity of S1P required MCDB (*A*, *C*). $n = 6$ in each group, $*P < 0.05$ from EGTA; $\#P < 0.05$ from EGTA:MCDB in *B* and EGTA:S1P in *C*.

treatment with S1P plus MCDB, the intensity of immunofluorescent staining of VE-cadherin at cell borders was greater at 10 min than with treatment of MCDB alone and was similar to immunofluorescent staining of control cell monolayers. Both treatments, S1P alone and S1P plus MCDB, resulted in the closure of most of the intercellular gaps. These microscopy and functional findings provide correlative evidence that S1P can rapidly close preexisting gaps between cells and increase endothelial electrical resistance in association with an absence of VE-cadherin at intercellular junctions.

Similar results were obtained by the addition of an antibody to the extracellular domain of VE-cadherin (Fig. 3) or gene silencing of VE-cadherin (Fig. 4). Addition to the culture medium of an extracellular VE-cadherin antibody resulted in a decrease in basal endothelial electrical resistance (Fig. 3) and a discontinuous appearance of VE-cadherin at intercellular junctions (data not shown) compared with the addition of normal rabbit IgG. S1P rapidly and transiently increased electrical resistance of cell monolayers incubated with the VE-cadherin antibody as well as the control IgG (Fig. 3). Transient trans-

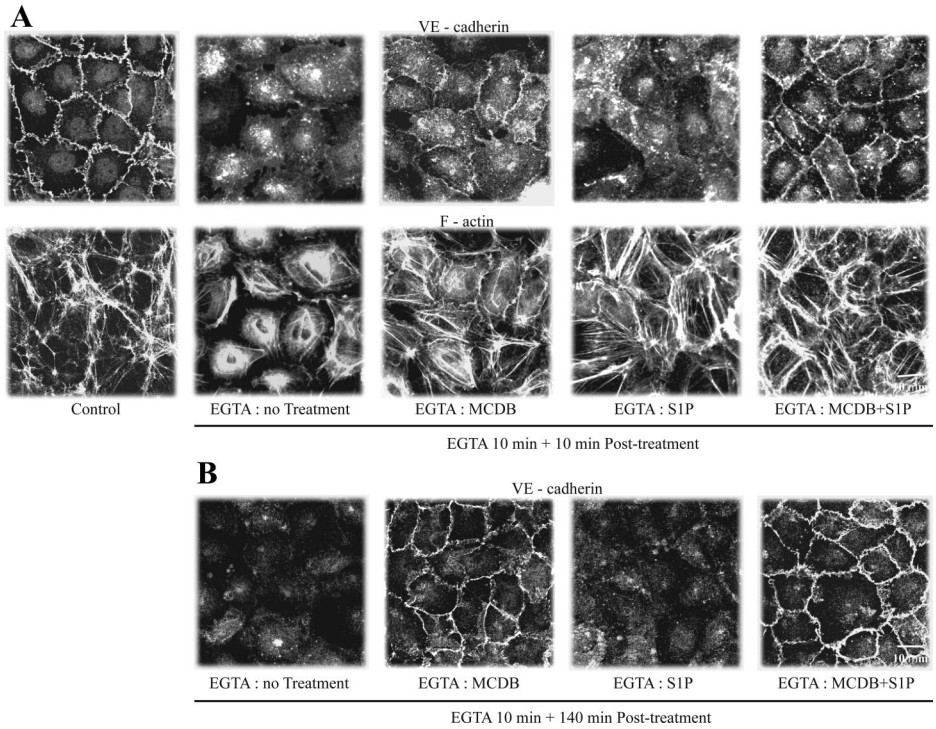

Fig. 2. S1P enhanced the junctional localization of vascular endothelial (VE)-cadherin and peripheral actin. EGTA protocol outlined in Fig. 1 was repeated for visualization of VE-cadherin and filamentous actin (F-actin) at cell periphery of same cells. *A* and *B*: representative micrographs of HUVEC monolayers at 10 (*A*) or 140 (*B*) min after treatment with MCDB, S1P, or S1P + MCDB. In fixed and permeabilized cell monolayers VE-cadherin was visualized by incubation with rabbit anti-human VE-cadherin polyclonal antibody and Alexa Fluor 594-labeled goat anti-rabbit secondary antibody, and F-actin was visualized with Alexa Fluor 488-labeled phalloidin. Note that treatment with S1P + MCDB increased presence of VE-cadherin at intercellular junctions (*A*), that S1P alone and S1P + MCDB reorganized actin to cell periphery (*A*), and that the presence of junctional VE-cadherin was maintained for 140 min only after treatment with MCDB or S1P + MCDB. Scale bars, 10 μm.

fection of VE-cadherin siRNA reduced the protein level of VE-cadherin by ~90% (Fig. 4*C*) and the localization of VE-cadherin at intercellular junctions [Fig. 4*A* (scrambled siRNA) vs. Fig. 4*B* (VE-cadherin siRNA)] within 48 h. As with the other two protocols, gene silencing of VE-cadherin caused a decrease in basal endothelial electrical resistance (Fig. 4*D*) that was apparent within 24 h and did not affect the rapid increase in endothelial electrical resistance induced by S1P. Moreover, S1P was still active in cell monolayers exposed to a combinatory protocol of reduction of VE-cadherin protein by gene silencing followed by chelation of extracellular Ca^{2+} with EGTA (Fig. 4*E*).

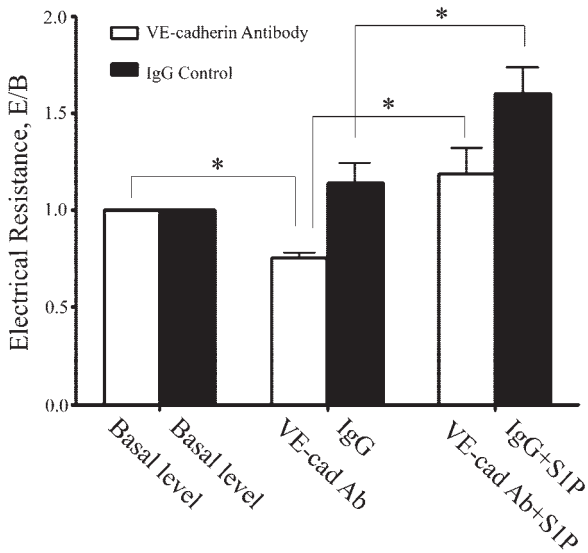

Fig. 3. S1P rapidly increased endothelial electrical resistance in presence of antibody to extracellular domain of VE-cadherin. Homophilic VE-cadherin binding was also disrupted by incubation with an antibody (Ab; CD144) to the extracellular domain of VE-cadherin. HUVEC monolayers were incubated for 60 min with VE-cadherin antibody or normal rabbit IgG and then treated with S1P. Note that endothelial electrical resistance [normalized to basal values (E/B)] decreased after 60-min administration of VE-cadherin antibody and that S1P increased electrical resistance (peak response) in both treated groups. $n = 4$ in each group. $^*P < 0.05$ vs. indicated group.

S1P augmented junctional localization of VE-cadherin. Within 10 min of treatment, S1P was observed to increase the localization of VE-cadherin at intercellular junctions (Fig. 2*A*). This observation was made only when S1P was administered in the presence of extracellular Ca^{2+}. After administration of EGTA (Fig. 2*A*), more VE-cadherin was present at intercellular junctions with treatment with S1P and MCDB, the latter to restore extracellular Ca^{2+}, compared with treatment with MCDB or S1P alone. This increased localization was also observed under normal cell culture conditions (see Fig. 6*B*).

Sustained increase in endothelial electrical resistance induced by S1P was associated with localization of VE-cadherin. With the EGTA protocol, there was a sustained increase in endothelial electrical resistance (Fig. 1, *A* and *C*; see also Figs. 4*E* and 7*B*), and VE-cadherin was localized to intercellular junctions (Fig. 2*B*) at 140 min after S1P was administered in combination with MCDB. Endothelial electrical resistance was also maintained for 140 min by S1P plus MCDB in cell monolayers transfected with a scrambled siRNA and then administered EGTA (Fig. 4*E*); VE-cadherin was localized to intercellular junctions in those cell monolayers (Fig. 4*F*, *top*). In contrast, treatment with S1P alone, without the addition of MCDB, induced only a transient increase in electrical resistance, because electrical resistance returned to the EGTA-only treated value by 140 min (Fig. 1, *A* and *C*), and at that time point junctional localization of VE-cadherin was much reduced (Fig. 2*B*). The activity of S1P was also transient in cell monolayers pretreated with the VE-cadherin antibody, which was not removed during the course of the experiment (data not

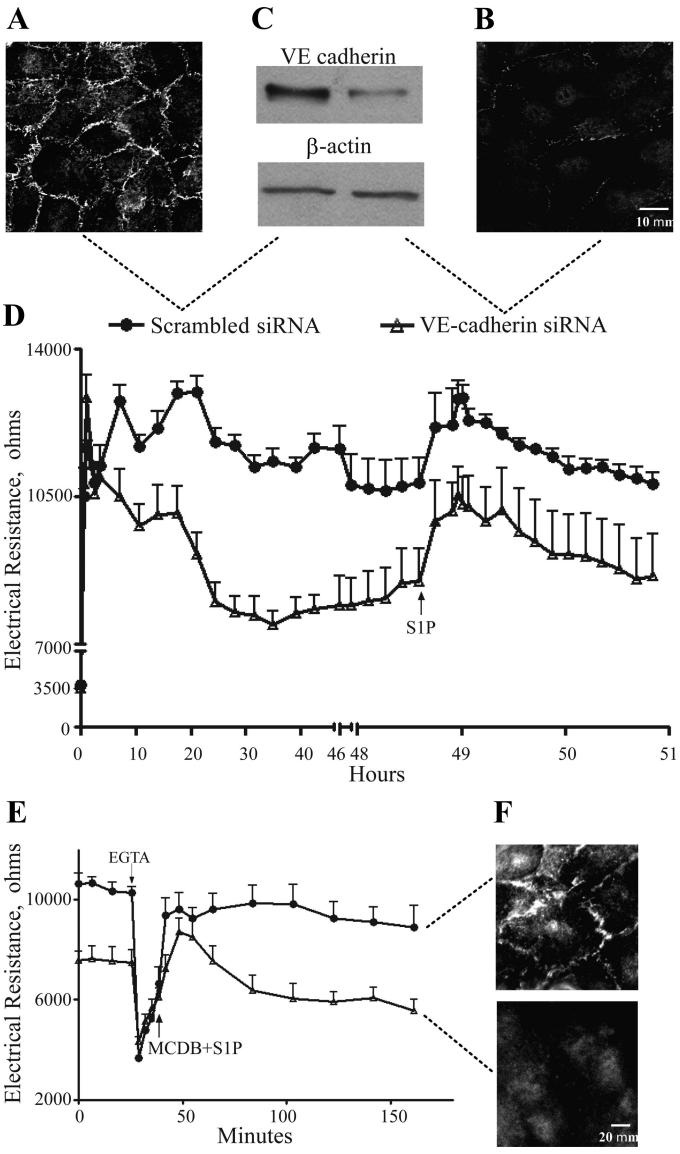

Fig. 4. S1P increased endothelial electrical resistance after gene silencing of VE-cadherin. HUVEC monolayers (90% confluence) were transiently transfected by electroporation with VE-cadherin small interfering RNA (siRNA) or scrambled siRNA. Transfected cells were seeded on 24-well culture dishes and incubated for 2 days until being used for microscopy (*A*, *B*) or Western blot (*C*) experiments or seeded on electrode cell-substrate impedance sensing (ECIS) wells for continuous measurement of electrical resistance (*D*). *A* and *B*: VE-cadherin was visualized at 48 h by incubation with CD144 antibody to VE-cadherin and Alexa Fluor 594-labeled goat anti-rabbit secondary antibody. *D*: continuous measurement of endothelial electrical resistance for ~48 h after electroporation of VE-cadherin siRNA or scrambled siRNA and after treatment with S1P (arrow); MCDB with 25% serum was replaced with serum-free MCDB at 46 h. *E*: EGTA was administered for 10 min to cell monolayers already transfected with either VE-cadherin siRNA or scrambled siRNA and then treated with S1P + MCDB (arrow). *F*: cells were viewed directly on ECIS wells at end of experiment by incubation with rabbit anti-human VE-cadherin polyclonal antibody and Alexa Fluor 594-labeled goat anti-rabbit secondary antibody. Note that S1P increased endothelial electrical resistance in both transfected groups (*D*) and that increased electrical resistance was maintained only in scrambled siRNA group in which VE-cadherin was localized to cell borders (*F*, *top*). $n = 5$ in each group. Scale bars, 10 (*A*, *B*) or 20 (*F*) μm.

shown). Furthermore, S1P activity was transient in those cell monolayers reduced in VE-cadherin protein by gene silencing followed by chelation of extracellular Ca^{2+} with EGTA (Fig. 4*E*). Immunofluorescent staining of VE-cadherin was much reduced at intercellular junctions at the end of the experiment in these cell monolayers (Fig. 4F, *bottom*). Therefore, the sustained increase in endothelial electrical resistance induced by S1P, with the EGTA protocol, appears to require VE-cadherin.

S1P induced cell spreading. Imaging of live cells with phase-contrast and DIC optics revealed that endothelial cells within a monolayer spread after the administration of S1P (Fig. 5). Administration of EGTA for 10 min increased the birefringence, indicative of a change in cell shape, of the cell monolayers as viewed by phase-contrast optics (Fig. 5*A*) and caused gaps with connecting strands to form between cells as viewed with DIC optics (Fig. 5*B*). Subsequent treatment for 10 min with S1P alone or in combination with MCDB resulted in cellular changes indicative of cell spreading, i.e., reduction of the birefringence (Fig. 5*A*), reduction of the connecting strands between cells, closure of intercellular gaps (Fig. 5*B*), appearance of flatter cells (Figs. 5*B*), and ridges between adjacent cells (Fig. 5*B*). Addition of MCDB alone to restore extracellular Ca^{2+} caused cell spreading and closure of intercellular gaps but to a much lesser extent than with S1P. These observations implicate cell spreading and the resultant closure of intercellular gaps as the mechanism for the S1P-induced rapid increase in electrical resistance of endothelial cell monolayers.

Latrunculin B inhibited S1P effects on electrical resistance and cell spreading. S1P is known to reorganize actin to the cell periphery (8). Visualization of actin filaments with phalloidin conjugated to Alexa Fluor 488 revealed in the present study that S1P also reorganized actin to the cell periphery in the presence of reduced VE-cadherin at intercellular junctions, resulting from administration of EGTA (Fig. 2*A*). To determine the role of actin in the barrier-enhancing activity of S1P, actin polymerization was blocked with latrunculin B. Pretreatment with latrunculin B for 30 min attenuated the increase in endothelial electrical resistance (Fig. 6*A*) and reorganization of peripheral actin (Fig. 6*B*) but had no effect on the increase in junctional VE-cadherin induced by S1P (Fig. 6*B*). Latrunculin B also prevented cell spreading induced by S1P. S1P reversed the EGTA-induced increases in birefringence (Fig. 6*C*) and gap formation (Fig. 6*D*) in cell monolayers pretreated with the vehicle DMSO, but not with latrunculin B.

Rho kinase inhibitor attenuated S1P effects on electrical resistance and cell spreading. Rho kinase and its downstream effectors influence cofilin, an actin-severing protein (8). Inhibition of cofilin by activated Rho kinase has been proposed to be responsible for the reorganization of peripheral actin induced by S1P (8). Pretreatment for 30 min with 5 μM Y-27632, a pharmacological inhibitor of Rho kinase, decreased basal endothelial electrical resistance and significantly attenuated the rapid increase in electrical resistance induced by S1P when administered either under normal conditions (Fig. 7*A*) or after EGTA treatment (Fig. 7*B*); Y-27632 at 1 μM had no effect in either condition (Fig. 7, *A* and *B*). In the EGTA protocol, addition of MCDB caused a small increase in endothelial electrical resistance, which slowly increased to the precontrol level (Fig. 7*B*), an observation similar to that depicted in Fig. 1*A*. Pretreatment with Y-27632 before the addi-

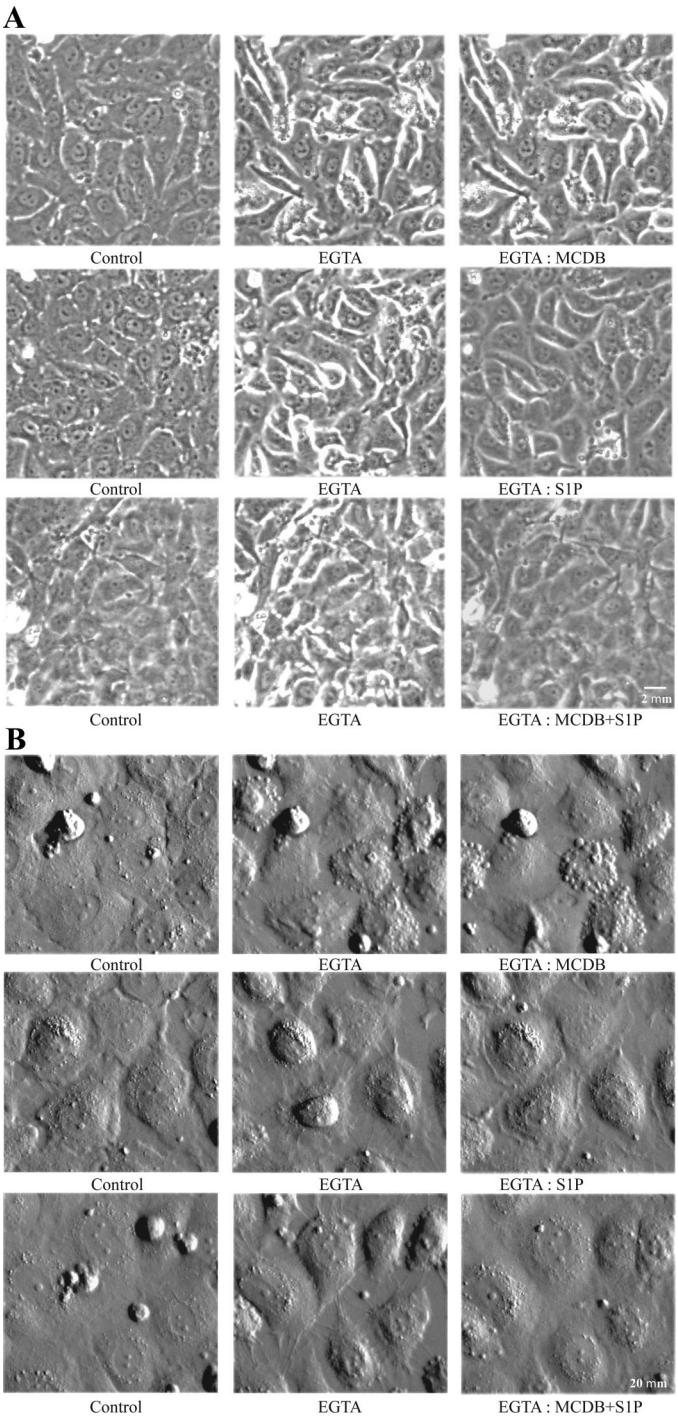

Fig. 5. S1P induced cell spreading. Cell spreading and closure of intercellular gaps of HUVEC monolayers were visualized with phase-contrast (*A*) and differential interference contrast (DIC; *B*) optics. Increased birefringence (*A*) and gaps with connecting strands between adjacent cells (*B*) were induced by 10-min incubation with EGTA (2 mM) to culture medium. HUVEC monolayers were then treated for 10 min with MCDB or S1P alone or S1P + MCDB. Note that S1P treatment without or with MCDB decreased birefringence (*A*) and induced cells to spread, resulting in closure of most of the intercellular gaps (*B*). Same group of cells is depicted in each row in *A* and *B*. Scale bars, 2 (*A*) or 20 (*B*) μm.

tion of EGTA also attenuated the decrease in birefringence, spreading of endothelial cells, and closure of intercellular gaps induced by S1P, as viewed by phase-contrast (Fig. 7*C*) and DIC (Fig. 7*D*) optics. Therefore, the findings with inhibitors of actin polymerization and Rho kinase suggest that S1P rapidly increases endothelial electrical resistance via an actin-dependent process that involves Rho kinase.

DISCUSSION

Two publications have demonstrated that S1P enhances the localization of the endothelial adherens junction proteins VE-cadherin and catenins within 30–60 min of treatment (9, 13). S1P, however, rapidly increases endothelial barrier function (8, 17), as noted by a peak increase in electrical resistance within 6–10 min. Whether VE-cadherin plays a significant role in this rapid activity of S1P was an intriguing question, especially after we observed that S1P enhanced the localization of VE-cadherin within 10 min of treatment. On the basis of experiments in which homophilic VE-cadherin binding was disrupted by three different mechanisms, cell monolayers were imaged with phase-contrast and DIC optics, and inhibitors of actin polymerization and Rho kinase were administered, we conclude that the rapid increase in endothelial electrical resistance induced by S1P occurs independently of homophilic VE-cadherin binding and requires cell spreading and Rho kinase. However, our initial findings suggest that the sustained activity of S1P demonstrated in the EGTA protocol requires VE-cadherin.

S1P induces the assembly of adherens junctions via activation of the small GTPases Rac1 and Rho (9, 13). Localization of VE-cadherin and α-, β-, and γ-catenins to intercellular junctions increased markedly and more VE-cadherin was demonstrated in the Triton X-100-insoluble (actin associated) fraction within 60 min in HUVECs treated with S1P. Inhibition of either Rho with C3 exoenzyme or Rac1 with dominant-negative N17Rac1 diminished the increased immunofluorescent staining of VE-cadherin at intercellular junctions (9). Similar increases in VE-cadherin and β-catenin were also observed at intercellular junctions within 30 min of S1P treatment (13). In the present study, we observed an increased immunofluorescent localization of VE-cadherin at intercellular junctions within 10 min of S1P treatment.

Since this 10-min time point temporally aligns with the rapid activity of S1P, we determined whether VE-cadherin is responsible for the rapid increase in endothelial electrical resistance induced by S1P. Homophilic VE-cadherin binding was disrupted by three different protocols, and all three protocols caused reduction in immunofluorescent localization of VE-cadherin at intercellular junctions, separation of adjacent endothelial cells, and a decrease in basal endothelial electrical resistance. The important finding was that S1P rapidly increased endothelial electrical resistance in all three protocols. After the administration of EGTA, the rapid increase in electrical resistance occurred when S1P was administered either without or with restoration of extracellular Ca^{2+} with MCDB. VE-cadherin was present at intercellular junctions in monolayers treated with MCDB alone and was increased with treatment of S1P plus MCDB, but much less VE-cadherin was observed at intercellular junctions after treatment with S1P alone. S1P was also effective in increasing endothelial electrical resistance

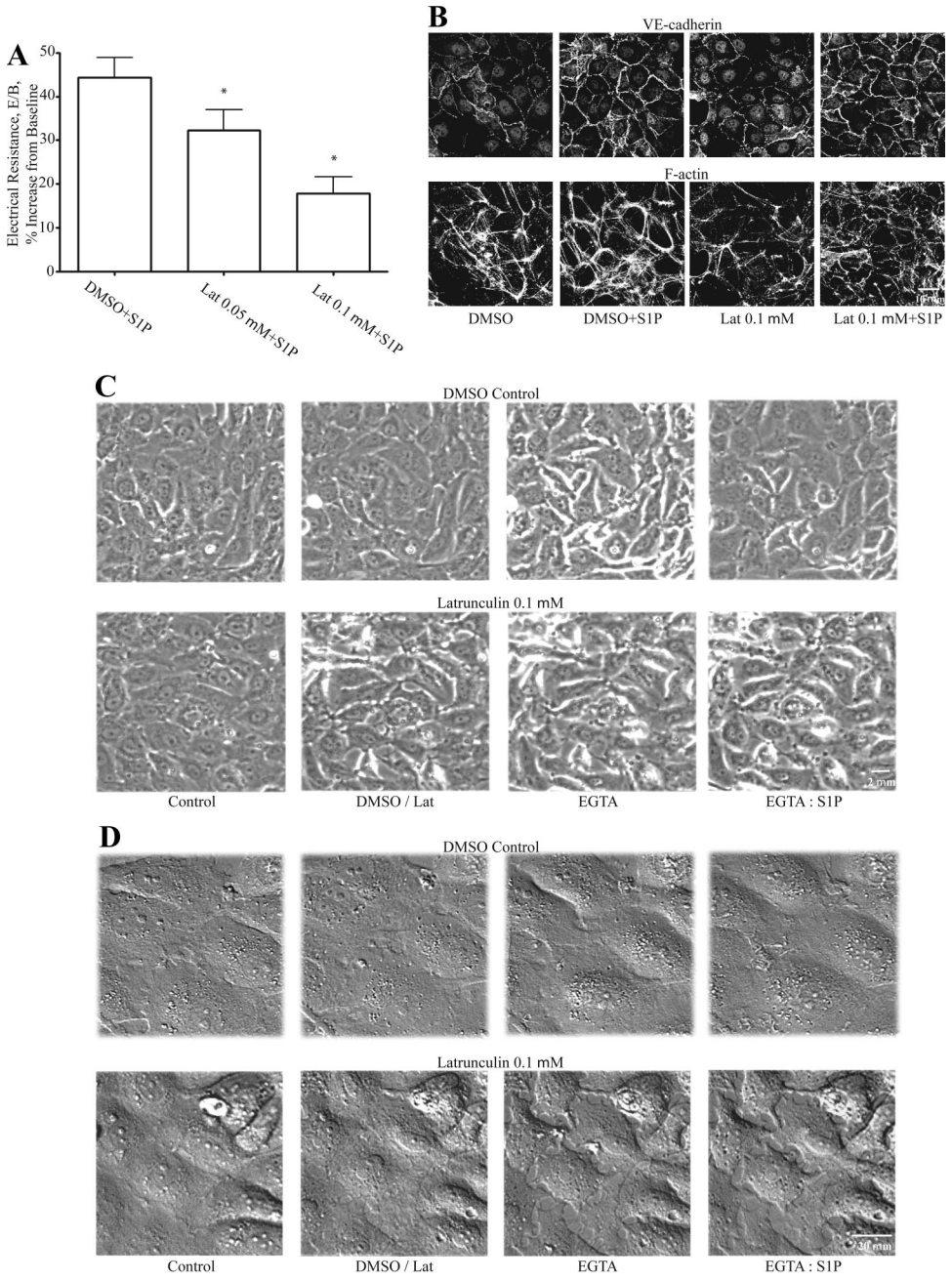

Fig. 6. Inhibitor of actin polymerization attenuated S1P-induced increase in endothelial electrical resistance and cell spreading. HUVEC monolayers were pretreated for 30 min with latrunculin B (Lat) to inhibit actin polymerization before treatment with S1P for 10 min. *A*: peak increases in electrical resistance, as normalized to basal values (E/B). *B*: VE-cadherin and actin were visualized, respectively, by incubation with rabbit anti-human VE-cadherin polyclonal antibody and Alexa Fluor 488-labeled goat anti-rabbit secondary antibody and Alexa Fluor 594-labeled phalloidin. Same group of cells is depicted in each column in *B*. *C* and *D*: same group of cells in each row was imaged with phase-contrast (*C*) or DIC (*D*) optics. EGTA was administered to disrupt homophilic VE-cadherin binding, resulting in formation of intercellular gaps. Note that latrunculin B attenuated increase in endothelial electrical resistance (*A*) and reorganization of F-actin to cell periphery (*B*), decrease in birefringence of cell monolayers (*C*), and cell spreading and closure of intercellular gaps (*D*) induced by S1P. Latrunculin B did not affect S1P-induced increase in localization of junctional VE-cadherin (*B*). $n = 5$ in each group in *A*. $^*P < 0.05$ vs. DMSO + S1P group. Scale bars, 10 (*B*), 2 (*C*), or 20 (*F*) μm.

after presumably interfering with homophilic VE-cadherin binding by incubation with an antibody to the extracellular domain of VE-cadherin or after VE-cadherin was reduced significantly by gene silencing. These findings support our conclusion that S1P rapidly increases endothelial electrical resistance independently of homophilic VE-cadherin binding.

The sustained increase in electrical resistance induced by S1P appears to require extracellular Ca^{2+} and the localization of VE-cadherin at intercellular junctions. After the administration of EGTA, the increased electrical resistance induced by S1P was sustained in cell monolayers containing junctional VE-cadherin. After EGTA, the sustained increase in electrical resistance induced by S1P required restoration of extracellular Ca^{2+} with MCDB, which was associated with the presence of VE-cadherin at intercellular junctions. Similarly, S1P maintained electrical resistance in cell monolayers containing junctional VE-cadherin after transfection with scrambled siRNA and the subsequent administration of EGTA. In contrast, treatment with S1P without replenishment of extracellular Ca^{2+} after EGTA or after reduction of VE-protein coupled with EGTA resulted in only a transient increase in electrical resistance, and junctional VE-cadherin was much reduced at the 140-min time point.

We next determined whether S1P induced cell spreading, because in the initial experiments S1P reorganized actin to the cell periphery and also appeared to reduce the width of intercellular gaps initially formed by EGTA. Cell spreading is also induced by cAMP-enhancing agents that are well known to rapidly tighten the endothelial barrier in association with reorganization of actin to the cell periphery (15, 22). S1P has been

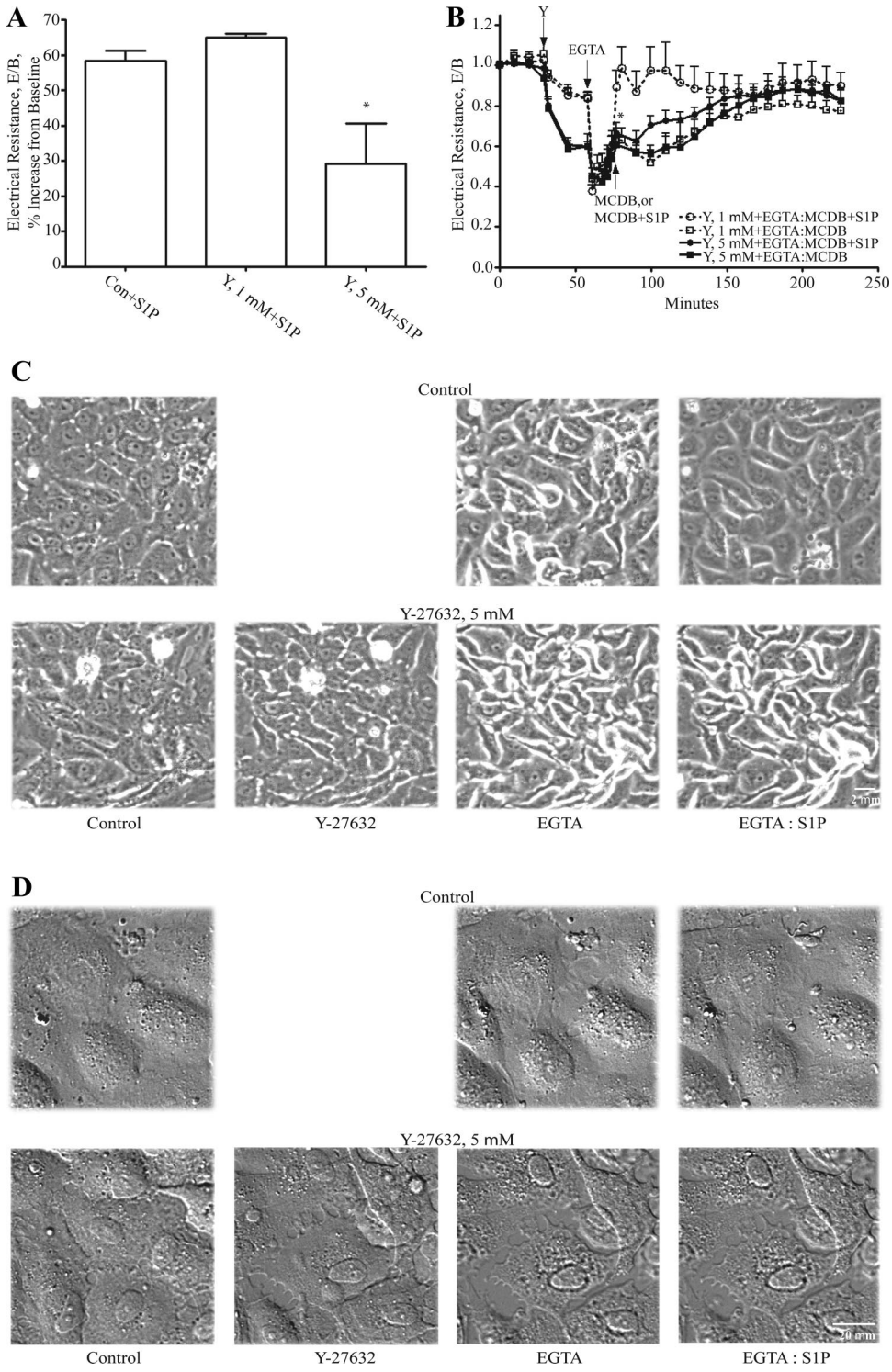

Fig. 7. Inhibitor of Rho kinase attenuated S1P-induced increase in endothelial electrical resistance and cell spreading. HUVEC monolayers were pretreated for 30 min with Y-27632 (Y; 1 and 5 μM), an inhibitor of Rho kinase, before treatment with S1P (*A*, *C*, *D*), MCDB alone (*B*), or S1P + MCDB (*B*). *A*: peak increases in electrical resistance, as normalized to basal values (E/B). *B–D*: EGTA was added to disrupt homophilic VE-cadherin binding and induce formation of intercellular gaps. Same group of cells in each row was imaged with phase-contrast (*C*) or DIC (*D*) optics. Note that Y-27632 at 5 μM attenuated increase in endothelial electrical resistance (*A*, *B*), decrease in birefringence of cell monolayers (*C*), and cell spreading and closure of intercellular gaps (*D*) induced by S1P. Y-27632 at 1 μM had no effect on these parameters. $n = 3$ in each group in *A* and 4 in each group in *B*. $^*P < 0.05$ vs. Control (Con) + S1P group (*A*) and Y 1 μM + EGTA:MCDB+S1P (*B*). Scale bars, 2 (*C*) or 20 (*D*) μm.

shown to induce membrane ruffling and cell spreading in single endothelial cells of human umbilical origin and to increase cell size (6, 18). S1P also formed lamellipodia and induced cell spreading of endothelial cells at the leading edge of wounded HUVEC monolayers, resulting in closure of the wound (25). In the present study, we observed by imaging with phase-contrast and DIC optics that S1P also induces spreading of endothelial cells grown as confluent monolayers. Treatment for 10 min with S1P without or with MCDB to restore extracellular Ca^{2+} caused cells to spread, resulting in closure of intercellular gaps initially formed by EGTA. These observations indicate that the rapid increase in electrical resistance across endothelial cell monolayers induced by S1P occurs via cell spreading and the subsequent closure of intercellular gaps. Although the above-mentioned formation of lamellipodia and subsequent closure of wounded HUVEC monolayers implicate the process of cell

spreading, the conditions (injury vs. EGTA-induced gap formation) and the signaling pathways are different. Wound closure by S1P was prevented by pretreatment with inhibitors of Src (PP2) and mitogen-activated protein kinase (U-0126), whereas the increased endothelial electrical resistance induced by S1P was not affected by PP2 or U-0126 (8). Similarly, we showed previously (7) that U-0126 did not block the increase in endothelial electrical resistance induced by platelet-conditioned medium, of which S1P has been suggested as the barrier-enhancing factor (20).

Garcia et al. (8) initially demonstrated that S1P remodeled actin to the cell periphery and that latrunculin B, an inhibitor of actin polymerization, or Y-27632, an inhibitor of Rho kinase, attenuated the S1P-induced increase in endothelial electrical resistance. We confirmed these findings and, in addition, demonstrated that S1P reorganized actin to the cell periphery after disruption of homophilic VE-cadherin binding with EGTA and that pretreatment with latrunculin B or Y-27632 (5 μM) attenuated actin reorganization and the cell spreading induced by S1P. Y-27632 also lowered basal endothelial electrical resistance in HUVEC monolayers. The preventative effects of Y-27632 may be explained by the ability of Rho kinase to inactivate cofilin, an actin-severing protein, via the phosphorylation of LIM kinase. Expression of wild-type cofilin has been reported to reduce the S1P-induced increases in peripheral actin and in endothelial electrical resistance (8). Rho kinase is also an effector for the small GTPase Rho, and activation of Rho has been implicated in the spreading of single endothelial cells by S1P (18) or of cells grown on type IV collagen (10). In these studies, inactivation of Rho with C3 exoenzyme blocked spreading of endothelial cells. The barrier-enhancing activity of S1P, therefore, appears to be dependent on the Rho-Rho kinase signaling pathway.

Rho kinase has also been implicated in loosening of the endothelial barrier. Y-27632 attenuated the activated neutrophil-induced increases in albumin permeability of porcine coronary venules and of cell monolayers derived from coronary venular endothelia and in cell tension of coronary venular endothelia (2). A similar attenuation of albumin permeability by Y-27632 was demonstrated in porcine coronary venules and coronary venular endothelia treated with vascular endothelial growth factor (23). Furthermore, transfection of constitutively active Rho kinase increased the permeability and endothelial cell tension in these two model systems (2). With regard to the effect of inhibition of Rho kinase on thrombin's ability to increase endothelial permeability, the findings are equivocal. Y-27632 prevented the increase in endothelial permeability in one study (27), but not in another study (3). Y-27632 per se enhanced the barrier function of cell monolayers derived from bovine pulmonary artery endothelial cells, as assessed by a size-selective permeability assay (3). In contrast, we show here that Y-27632 decreased the endothelial barrier function of HUVEC monolayers, as assessed by a decrease in endothelial electrical resistance. From the findings of the above-described studies and the present study, it is apparent that the outcome of activation of the Rho kinase signaling pathway is varied. One possibility is that the cellular targets downstream of Rho kinase are different for various mediators or for different cell types and that separate or parallel pathways differentially influence endothelial barrier function.

ACKNOWLEDGMENTS

We thank the Confocal Microscopy and Image Analysis Core Facility at West Virginia University Health Sciences for the use of the confocal microscope. We also thank the research laboratory of Dr. Scott Weed (West Virginia University School of Medicine) for the use of the Nucleofector I device.

GRANTS

This work was supported by National Heart, Lung, and Blood Institute Grants HL-68079 (F. L. Minnear), HL-52406 (P. A. Vincent), and HL-45788 (R. B. Wysolmerski) and by an American Heart Association scientific development grant (C. Hu).

REFERENCES

1. **Bazzoni G, Dejana E.** Endothelial cell-to-cell junctions: molecular organization and role in vascular homeostasis. *Physiol Rev* 84: 869–901, 2004.
2. **Breslin JW, Sun H, Xu W, Rodarte C, Moy AB, Wu MH, Yuan SY.** Involvement of ROCK-mediated endothelial tension development in neutrophil-stimulated microvascular leakage. *Am J Physiol Heart Circ Physiol* 290: H741–H750, 2006.
3. **Carbajal JM, Gratrix ML, Yu CH, Schaeffer RC Jr.** ROCK mediates thrombin's endothelial barrier dysfunction. *Am J Physiol Cell Physiol* 279: C195–C204, 2000.
4. **Corada M, Liao F, Lindgren M, Lampugnani MG, Breviario F, Frank R, Muller WA, Hicklin DJ, Bohlen P, Dejana E.** Monoclonal antibodies directed to different regions of vascular endothelial cadherin extracellular domain affect adhesion and clustering of the protein and modulate endothelial permeability. *Blood* 97: 1679–1684, 2001.
5. **Corada M, Mariotti M, Thurston G, Smith K, Kunkel R, Brockhaus M, Lampugnani MG, Martin-Padura I, Stoppacciaro A, Ruco L, McDonald DM, Ward PA, Dejana E.** Vascular endothelial-cadherin is an important determinant of microvascular integrity in vivo. *Proc Natl Acad Sci USA* 96: 9815–9820, 1999.
6. **Endo A, Nagashima KI, Kurose H, Mochizuki S, Matsuda M, Mochizuki N.** Sphingosine 1-phosphate induces membrane ruffling and increases motility of human umbilical vein endothelial cells via vascular endothelial growth factor receptor and CrkII. *J Biol Chem* 277: 23747–23754, 2002.
7. **Gainor JP, Morton CA, Roberts JT, Vincent PA, Minnear FL.** Platelet-conditioned medium increases endothelial electrical resistance independently of cAMP/PKA and cGMP/PKG. *Am J Physiol Heart Circ Physiol* 281: H1992–H2001, 2001.
8. **Garcia JGN, Liu F, Verin AD, Birukova A, Dechert MA, Gerthoffer WT, Bamburg JR, English D.** Sphingosine 1-phosphate promotes endothelial cell barrier integrity by Edg-dependent cytoskeletal rearrangement. *J Clin Invest* 108: 689–701, 2001.
9. **Lee MJ, Thangada S, Claffey KP, Ancellin N, Liu CH, Kluk M, Volpi M, Sha'afi RI, Hla T.** Vascular endothelial cell adherens junction assembly and morphogenesis induced by sphingosine-1-phosphate. *Cell* 99: 301–312, 1999.
10. **Masiero L, Lapidos KA, Ambudkar I, Kohn EC.** Regulation of the RhoA pathway in human endothelial cell spreading on type IV collagen: role of calcium influx. *J Cell Sci* 112: 3205–3213, 1999.
11. **McVerry BJ, Garcia JG.** Endothelial cell barrier regulation by sphingosine 1-phosphate. *J Cell Biochem* 92: 1075–1085, 2004.
12. **McVerry BJ, Peng X, Hassoun PM, Sammani S, Simon BA, Garcia JGN.** Sphingosine 1-phosphate reduces vascular leak in murine and canine models of acute lung injury. *Am J Respir Crit Care Med* 170: 987–993, 2004.
13. **Mehta D, Konstantoulaki M, Ahmmed GU, Malik AB.** Sphingosine 1-phosphate-induced mobilization of intracellular Ca^{2+} mediates Rac activation and adherens junction assembly in endothelial cells. *J Biol Chem* 280: 17320–17328, 2005.
14. **Mehta D, Malik AB.** Signaling mechanisms regulating endothelial permeability. *Physiol Rev* 86: 279–367, 2006.
15. **Minnear FL, DeMichele MAA, Moon DG, Rieder CL, Fenton JW II.** Isoproterenol reduces thrombin-induced pulmonary endothelial permeability in vitro. *Am J Physiol Heart Circ Physiol* 257: H1613–H1623, 1989.
16. **Minnear FL, Patil S, Bell D, Gainor JP, Morton CA.** Platelet lipid(s) bound to albumin increases endothelial electrical resistance: mimicked by LPA. *Am J Physiol Lung Cell Mol Physiol* 281: L1337–L1344, 2001.

17. **Minnear FL, Zhu L, He P.** Sphingosine 1-phosphate prevents platelet-activating factor-induced increase in hydraulic conductivity in rat mesenteric venules: pertussis toxin sensitive. *Am J Physiol Heart Circ Physiol* 289: H840–H844, 2005.
18. **Paik JH, Chae SS, Lee MJ, Thangada S, Hla T.** Sphingosine 1-phosphate-induced endothelial cell migration requires the expression of EDG-1 and EDG-3 receptors and Rho-dependent activation of $\alpha_v\beta_3$- and β_1-containing integrins. *J Biol Chem* 276: 11830–11837, 2001.
19. **Peng X, Hassoun PM, Sammani S, McVerry BJ, Burne MJ, Rabb H, Pearse D, Tuder RM, Garcia JGN.** Protective effects of sphingosine 1-phosphate in murine endotoxin-induced inflammatory lung injury. *Am J Respir Crit Care Med* 169: 1245–1251, 2004.
20. **Schaphorst KL, Chiang E, Jacobs KN, Zaiman A, Natarajan V, Wigley F, Garcia JG.** Role of sphingosine-1 phosphate in the enhancement of endothelial barrier integrity by platelet-released products. *Am J Physiol Lung Cell Mol Physiol* 285: L258–L267, 2003.
21. **Shuster CB, Herman IM.** The mechanics of vascular cell motility. *Microcirculation* 5: 239–257, 1998.
22. **Stelzner TJ, Weil JV, O'Brien RF.** Role of cyclic adenosine monophosphate in the induction of endothelial barrier properties. *J Cell Physiol* 139: 157–166, 1989.
23. **Sun H, Breslin JW, Zhu J, Yuan SY, Wu MH.** Rho and ROCK signaling in VEGF-induced microvascular endothelial hyperpermeability. *Microcirculation* 13: 237–247, 2006.
24. **Tschugguel W, Zhegu Z, Gajdzik L, Maier M, Binder BR, Graf J.** High precision measurement of electrical resistance across endothelial cell monolayers. *Pflügers Arch* 430: 145–147, 1995.
25. **Vouret-Craviari V, Bourcier C, Boulter E, van Obberghen-Schilling E.** Distinct signals via Rho GTPases and Src drive shape changes by thrombin and sphingosine-1-phosphate in endothelial cells. *J Cell Sci* 115: 2475–2484, 2002.
26. **Wallenstein S, Zucker CL, Fleiss JL.** Some statistical methods useful in circulation research. *Circ Res* 47: 1–9, 1980.
27. **Wojciak-Stothard B, Potempa S, Eichholtz T, Ridley AJ.** Rho and Rac but not Cdc42 regulate endothelial cell permeability. *J Cell Sci* 114: 1343–1355, 2001.